Solid-State Electronics Vol. 31, No. 12, pp. 1733–1742, 1988
Printed in Great Britain.

0038-1101/88 $3.00 + 0.00

DEEP LEVEL TRANSIENT FOURIER SPECTROSCOPY (DLTFS)—A TECHNIQUE FOR THE ANALYSIS OF DEEP LEVEL PROPERTIES

S. WEISS and R. KASSING
Institut für Technische Physik, Universität Kassel, D-3500 Kassel, F.R.G.

(*Received* 6 *April* 1988; *in revised form* 20 *June* 1988)

Abstract—The advantages of a DLTS method—the DLTFS method—are presented. In this technique the capacitance–time transients are digitalized, and the discrete Fourier coefficients are formed via numerical Fourier transformation. These coefficients can be used to calculate amplitude and time constant of the transients for discrete trap levels in various ways, thus giving control of the results. This permits automatic control of measuring parameters (e.g. choice of period width and temperature values), automatic evaluation during measurement (e.g. impurity concentration, activation energy and capture cross section), and high measuring accuracy. In contrast to the usual DLTS technique a temperature dependence of the amplitude, leading to errors especially in CC-DLTS and current-DLTS measurements, does not present a source of error. The good noise suppression is a further advantage of the DLTFS method.

NOTATION

A	amplitude of the transient
a_n	nth Fourier cosine coefficient
B	offset of the transient
b_n	nth Fourier sine coefficient
C	capacity
c_n	nth complex Fourier coefficient
E_C	energy level of the conduction band
E_F	Fermi level
E_T	energy level of the trap center
N_S	shallow donor concentration
N_T	trap concentration
T	temperature
T_W	period width
t	time
t_0	time between end of charging pulse and start of measurement
t_w	time window
Δt	sampling interval
τ	time constant

1. INTRODUCTION

The DLTS method is the most sensitive measuring method to determine characteristic electrical properties of deep levels in semiconductors. The method is based on measurements of capacitance transients of depletion layers during impurity charge transfer. It supplies concentration N_T, energetic position E_C–E_T, capture cross section σ, and, under certain circumstances, the entropy factor of deep levels[1–7]. With the evaluation method used predominantly[2] these data are obtained by forming the difference $\Delta C = C(t_1) - C(t_2)$ of the capacitances measured at two given times t_1 and t_2 as a function of temperature. For a discrete level, ΔC shows a maximum at a temperature T_{max}, where the emission time constant τ_e of the observed level is identical with the rate window t_w, i.e.

$$\tau_e(T_{max}) = t_w = (t_2 - t_1)/\ln(t_2/t_1). \quad (1)$$

Variation of the rate window t_w yields a relation $\tau_e(T)$ from which the data needed can be obtained via an Arrhenius plot. In the following this method, which was introduced by Lang, will be called conventional DLTS method. In this paper a new DLTS method called DLTFS (Deep Level Transient Fourier Spectroscopy) will be presented. It is characterized by the following four features:

(a) N measuring values are sampled from a capacitance transient. From these values discrete Fourier coefficients are formed by numerical Fourier transformation.

(b) From these coefficients the time constant and amplitude for each transient can be calculated immediately. Because these values can be calculated in several ways, and because specific relations between the coefficients are characteristic for different signal forms, a simultaneous examination of the results is possible.

(c) As the determination of the time constant is possible during the DLTFS measurement a program is developed, which controls the measurement by optimizing the parameters like temperature, measurement time, amplification etc.

(d) Due to the foregoing arguments (b) and (c) it is possible to adjust the period width T_W for every temperature computer controlled to the capacitance transients. This is of great advantage in the DLTFS method and of great importance with respect to noise suppression and measuring accuracy.

The Fourier transformation for DLTS mea-

surements was also used in [5–7]. One difference between these methods and our DLTFS is the automatic control of the results, allowing completely computer controlled measurement as well as adjustment of the period width to the capacitance transient, as already discussed. Moreover these methods are limited to separated discrete trap levels whereas the DLTFS theory is also developed for the separation of two overlapping discrete levels, as well as to investigate the charge transfer of interface states and the generation of minority carriers.

2. THEORY OF THE DLTFS-EVALUATION

In the following we assume a digital system, which scans the analog signal $f(t)$ with an analog-digital-converter (ADC) in N discrete equidistant times $k\Delta t$, $k = 0,1,\ldots,N-1$. Δt is the sampling interval. For $f(t)$ we postulate periodicity. The period width $T_W = N\Delta t$ contains N intervals with the $N+1$ real values $f_0,\ldots,f_N$.

For the subsequent comparison of measured and calculated values the following definitions are relevant:

(a) Continuous (analytical) Fourier coefficients c_n of the Fourier series (the continuous Fourier transformation, as used in Ref. [6], leads to errors because the time limited measuring time is not considered):

$$c_n = \frac{1}{T_W}\int_0^{T_W} f(t)\exp(-in\omega t)\,dt, \quad n \in Z \tag{2}$$

with

$$\omega = \frac{2\pi}{T_W}.$$

In case $f(t)$ is real, then the cosine coefficients a_n and the sine coefficients b_n are real, too, and represent real and imaginary parts of c_n:

$$c_n = \tfrac{1}{2}(a_n - ib_n), \quad n \geqslant 0 \tag{3}$$

(b) Discrete (numerical) Fourier Transform (DFT):

$$F_n = \sum_{k=0}^{N-1} f_k \exp(-2\pi ink/N), \qquad n = 0,1,\ldots,N-1. \tag{4}$$

As the sampling values are real, only $N/2$ independent F_n exist. The following relation exists between DFT and discrete Fourier coefficients c_n^D:

$$F_n = Nc_n^D. \tag{5}$$

The exact reconstruction of a continuous time signal $f(t)$, using discrete sampling values, is only possible if $f(t)$ is spectrally limited, and if the sampling frequency $1/\Delta t$ is more than twice the highest frequency of $f(t)$ (sampling theorem). The Nyquist frequency is half the sampling frequency. Spectral overlaps (aliasing effect) occur if the sampling theorem is not fulfilled.

Equation (4) represents the exact numerical integration according to the trapezium rule only if $f_0 = f_N$. Without this restriction the numerical integration rule takes the following form:

$$F_n = \frac{f_0}{2} + \sum_{k=1}^{N-1} f_k \exp(-2\pi ink/N) + \frac{f_N}{2}. \tag{6}$$

If the function shows a discontinuity at the scan limit, i.e. $f_0 \neq f_N$, then a correction is necessary if discrete and continuous coefficients are to be compared. This fact was not considered in Refs [5,6]. For the analytical case the peripheral points $f(0)$ and $f(T_W)$ are null sets. To avoid executing the correction for each F_n, f_0 can be defined as follows for the input values of the DFT:

$$f_0' := \frac{f_0 + f_N}{2}. \tag{7}$$

Numerical execution of the DFT can be done most efficiently with the FFT (Fast Fourier Transform) algorithm. The FFT produces the entire discrete frequency spectrum, but it cannot be used to calculate a few specific coefficients, only. However, as few coefficients are sufficient to determine the time constant, an algorithm was developed for the relevant coefficients from zeroth to fourth order, which is characterized by high calculating speed.

The general idea of the DLTFS method is as follows: N measuring values are sampled from a capacitance transient, and the discrete Fourier coefficients c_n^D are formed by numerical Fourier transformation.

Based on an adequate theory for the charging of deep levels a certain time dependence of the transient is assumed. This function is developed into a Fourier series, and its continuous coefficients c_n are calculated.

Assuming that the numerical coefficients originate from just this postulated function, the free parameters of the function can be determined by a comparison of the numerical and the analytical coefficients, usually in several ways.

Additionally, it is immediately possible to check the basic theory by an appropriate selection of the number of Fourier coefficients. As each coefficient contains information about the entire transient, specific ratios of some coefficients are characteristic for different signal forms.

Generally it would not be reasonable to use the entire frequency spectrum quantitatively for the evaluation. Starting with the assumption of a low-frequency active signal being overlapped by high-frequency noise signals, usually only the lowest orders will be evaluated.

In most cases it is favourable to adjust optimally the period width for each transient.

This principle has the additional advantage to avoid sampling errors. For example the finite observation time will be of no importance because we integrate up to $t = T_W$ for both, the numerical as well

as the analytical case. Further, the non-periodicity of the scan-limit can be corrected for the coefficients, according to eqn (7). Thirdly, as neither the analog signals are reconstructed by the Fourier series nor the sampling values filtered, Gibbs Phenomena is of no relevance and observance of the sampling theorem of insignificant importance. The differences between continuous and discrete coefficients are small for the first orders of the functions considered. The sampling theorem, however, has to be considered to avoid influences of the aliasing effect.

3. DLTFS THEORY AND SIMULATIONS FOR AN EXPONENTIAL LAW OF TIME

3.1. Coefficients of the exponential function

The following discusses a real exponential law of time:

$$f(t) = A \exp[-(t + t_0)/\tau] + B, \tag{8}$$

where A is the amplitude, B the offset, τ the time constant and $-t_0$ the time at the end of charging pulse. For the real function of eqn (8) following Fourier coefficients are obtained:

$$a_0 = \frac{2A}{T_W} \exp(-t_0/\tau) \times [1 - \exp(-T_W/\tau)]\tau + 2B \tag{9}$$

$$a_n = \frac{2A}{T_W} \exp(-t_0/\tau) \times [1 - \exp(-T_W/\tau)] \frac{1/\tau}{1/\tau^2 + n^2\omega^2} \tag{10}$$

$$b_n = \frac{2A}{T_W} \exp(-t_0/\tau) \times [1 - \exp(-T_W/\tau)] \frac{n\omega}{1/\tau_2 + n^2\omega^2}. \tag{11}$$

Figure 1 shows a_n and b_n for two different time constants. While the cosine coefficients a_n of higher order are always smaller than those of lower order, the reverse can occur for the sine coefficients b_n.

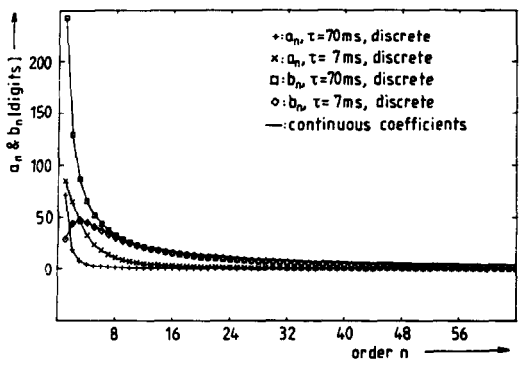

Fig. 1. Discrete and continuous Fourier coefficients of two exponential functions for $N = 128$, $A = 1000$, $\Delta t = 1$ ms and $t_0 = \Delta t$.

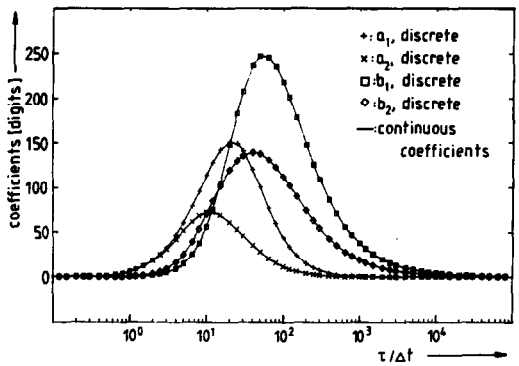

Fig. 2. Development of coefficients of 1st and 2nd order for $N = 128$, $A = 1000$ and $t_0 = \Delta t$.

Because in general the coefficients drop sharply with increasing order, and the deviation from analytical value increases due to the spectral overlap of higher frequencies, only the first few orders are used.

Figure 2 shows the variation of the coefficients of 1st and 2nd order with respect to $\tau/\Delta t$. As the exponential function is determined by the normalized relation $\tau/\Delta t$ and not by τ, $\tau/\Delta t$ was chosen as x-axis. The squares and crosses mark the discrete coefficients, while the dots of the corresponding continuous coefficients were connected by straight lines. From eqns (10) and (11) we can get the following relations to check whether the transient is exponentional:

(a) $a_2 < a_1 < 4a_2$,

(b) $b_2/2 < b_1 < 2b_2$,

(c) $\frac{b_1}{a_1}\frac{a_2}{b_2} = \frac{1}{2}$.

The amplitude of the signal, and consequently the concentration of deep centers, can be calculated from each coefficient in eqns (10) and (11) e.g.:

$$A = \frac{T_W}{2} b_n \frac{\exp(t_0/\tau)}{[1 - \exp(-T_W/\tau)]} \frac{1/\tau^2 + n^2\omega^2}{n\omega}. \tag{12}$$

At the start of measurement we take $t = 0$. In an analytical integration one must always integrate from $t = 0$ up to $t = T_W$ because the numerical integration takes place within these limits as well. Would $-t_0$ (end of charging pulse) be selected as time zero, the analytical and numerical coefficients would not have the same phase and would therefore not be comparable. This aspect has not been taken into account in Ref. [5].

3.2. Determination of time constant

The time constant can be best obtained from the ratio of two coefficients. There exist three principally

different possibilities:

$$\tau(a_n, a_k) = \frac{1}{\omega}\sqrt{\frac{a_n - a_k}{k^2 a_k - n^2 a_n}} \tag{13a}$$

$$\tau(b_n, b_k) = \frac{1}{\omega}\sqrt{\frac{kb_n - nb_k}{k^2 nb_k - n^2 kb_n}} \tag{13b}$$

$$\tau(a_n, b_n) = \frac{1}{n\omega}\frac{b_n}{a_n}. \tag{13c}$$

It is of considerable advantage that eqn (13) uses only ratios of coefficients and neither amplitude nor offset. Hence a temperature dependence of the amplitude does not present a source of error.

If the offset is known, τ can also be calculated from a_0:

$$\tau(a_0) = \left(\frac{a_0}{2} - B\right)\frac{T_W \exp(t_0/\tau)}{A[1 - \exp(-T_W/\tau)]}. \tag{14}$$

For this an approximate knowledge of the time constant is necessary, which can be obtained from eqn (13).

For $N = 1024$ Fig. 3 shows the percentage deviation of calculated $\tau/\Delta t$-values from those given. According to this $\tau(a_1, b_1)$ is most often found closest to the exact value. The cause for the error is to be found mainly in the difference between continuous and discrete coefficients because the sampling theorem is violated.

The data shown in Fig. 3 contain already the correction for the peripheral values as obtained through eqn (7). Without this correction the evaluation would be limited to a substantially narrower $\tau/\Delta t$-range.

Additionally to this method it is possible to evaluate the emission time constant—analogous to the DLTS method—via the maxima of the Fourier temperature curves.

3.3. *Quantization errors*

The preceding considerations did not take into account a main source of error of a real digital system, i.e. the discretization of the amplitude axis by the ADC. The effect of quantization noise by the DLTFS method is less than the DLTS method because this noise is filtered by the Discrete Fourier Transformation.

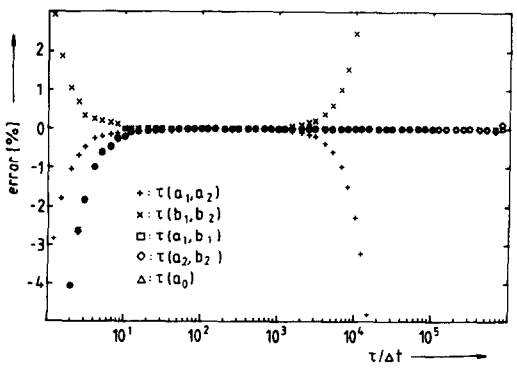

Fig. 3. Error in the τ-calculation for real sampling values for $N = 1024$ and $t_0 = \Delta t$.

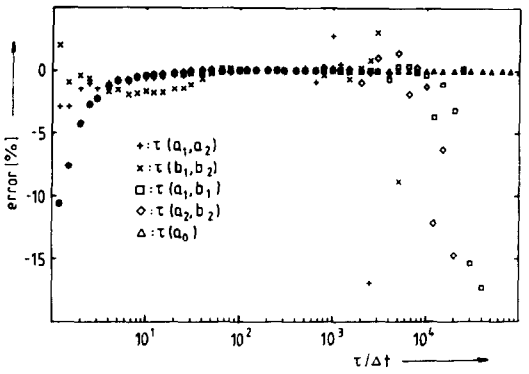

Fig. 4. Error in the τ-calculation for $N = 1024$, $A = 1000$ digits and $t_0 = \Delta t$, using quantized sampling values.

Figure 4 shows the influence of this quantization noise on the τ-calculation for an amplitude of 1000 digits, corresponding to a resolution of approximately 10 Bit. For reasons of clarity only those values are shown whose errors remain within a certain limit.

Figure 4 shows quite clearly that in comparison to Fig. 3 the $\tau/\Delta t$-range to be evaluated is strongly limited. As in Fig. 3, the best results are produced mainly by $\tau(a_1, b_1)$. The curves can be explained by the coefficient development and by eqn (13):

(a) In the medium $\tau/\Delta t$-range the error due to the amplitude discretization is minimal because at $\tau/\Delta t \approx 140$ the transient falls below the sensitivity of the ADC.

(b) $\tau(a_1, a_2)$ and $\tau(b_1, b_2)$ are calculated by taking differences of coefficients. Because the absolute error adds up the results deteriorate as the smaller these differences are. For small and large $\tau/\Delta t$-relations numerator or denominator in eqns (13a) and (13b) tend towards zero.

(c) At $\tau(a_1, b_1)$ and $\tau(a_2, b_2)$ only the percentage error adds up.

(d) The apparently very good results of $\tau(a_0)$, especially for large $\tau/\Delta t$-relations, ought to be considered with caution, because here knowledge of the offset is necessary. For a number of measurements this value cannot be determined exactly.

(e) Even with undistorted signals evaluation of higher frequency components leads to worse results due to the larger influence of the aliasing effect and the quantization. For the low $\tau/\Delta t$-range, however, the corresponding calculations can be more advantageous. For coefficients of higher order the behaviour described in eqn (13a) and (13b) exert a much stronger influence, especially when k/n $(n < k)$ is small. For example, the ratio of b_7 and b_8 changes only between 7/8 and 8/7.

The agreement between calculated and postulated $\tau/\Delta t$-range to be evaluated, depends on the resolution of the ADC as well as on the number of measuring values.

All other errors are largely negligible in comparison to the quantization error. The aliasing effect (noise-free transients assumed) presents only a minor limitation of the evaluation in reality.

Figures 3 and 4 confirm that good control of results is possible. If the different τ-calculations deviate strongly from the exact values then they are also different from each other.

4. SIMULATION OF MEASUREMENTS

4.1. One discrete level

Measurements were simulated to determine the consequences of discretization of the amplitude and of noise interference of the transient on estimation of the charcteristic quantities of the trap level. For this purpose we assumed a deep level approximately comparable to the gold-donor level in p-type Si with an activation energy of 0.36 eV and a capture cross section of $4 \times 10^{-13}\,\mathrm{cm}^2$. These quantities were used to calculate the quantized sampling values of corresponding transients for various temperatures. These transients in turn were used to calculate the numerical Fourier coefficients. These were then used to determine the emission time constant.

For the evaluation of all τ-values the same temperature range marked by straight lines in Fig. 5 was used. In this simulation the amplitude of the transient reached 250 digits only. Evaluation of the $\tau(a_1, b_1)$-values yields the activation energy with an error of less than 0.2%, the capture cross section with an error of 2%. If the same range is evaluated for $\tau(b_1, b_2)$, the results are not so good.

In analogy to the calculation of the time constant the agreement between preset and calculated values of activation energy and capture cross section depends on amplitude (ADC-resolution) and number of measuring values. By the DLTS method the emission time is not obtained directly from the transient but from the maxima for various rate windows. The

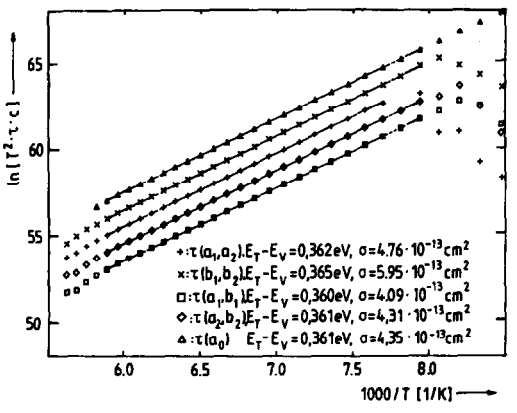

Fig. 5. Arrhenius plot at a fixed period width with $N = 1024$, $\Delta t = 1$ ms, $A = 250$ digits (equals a resolution of approximately 8 bit); $\tau(a_2, b_2)$, $\tau(a_1, a_2)$, $\tau(b_1, b_2)$ and $\tau(a_0)$ are displaced parallel.

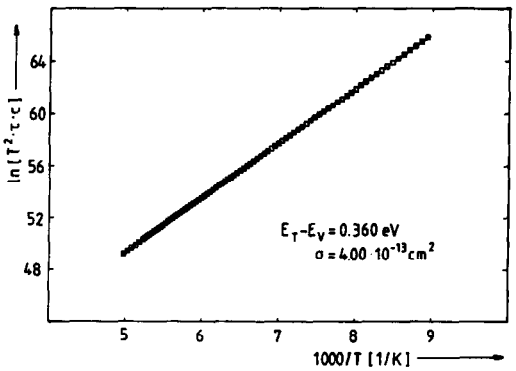

Fig. 6. Arrhenius plot at variable setting of period width.

DLTFS-method, on the other hand, enables one to judge the development of the function already during measurement. The following will outline this.

The first step ascertains by comparison of coefficients whether an exponential function exists. In the next step the point of time t_s is calculated where the quantized transient attains the equilibrium value. The relation t_s/T_W determines the location of the transient with respect to the period width chosen. For different t_s/T_W-ranges specific relations of the individual τ-calculation emerge. Depending on range and amplitude certain tolerances are permitted for the differences of τ-calculations. Simultaneously the optimum τ-value is selected. Further, each coefficient can be calculated analytically and compared to the numerical coefficient. All estimates are assigned a "quality"-number. For evaluation purposes it is then possible to select data of a certain "quality". Hence, revision of the results of the Arrhenius plot is not necessary.

To obtain values as accurate as possible for the characteristic quantities of the trap level it is necessary to sweep a large temperature range. As τ/T_W is measured, Δt or N can be varied to adapt the period width to the transient, to obtain $t_s/T_W \approx 1$. Figure 6 shows such a simulated measurement. Selection of the τ-values was performed according to their "quality" defined above and not with regard to their deviation from the straight lines of the Arrhenius plot. Using a maximum period width of 20 s, and a shortest sampling interval of 20 μs, the τ-range to be evaluated is by 3 orders of magnitude larger than that in Fig. 5. A variable period width is also of great advantage for noise suppression.

4.2. Overlapping of two exponential functions

If the measured signal consists of two exponential terms with similar time constants larger errors can occur in the determination of τ. To show this more clearly, measurements were simulated based on DLTS measurements of n-GaAs. Thus, we assume activation energies of 0.27 and 0.36 eV, capture cross sections of 2×10^{-14} and $5 \times 10^{-13}\,\mathrm{cm}^2$, and amplitudes of 1000 and 2000 digits. Figure 7 shows the Fourier temperature curves of such a simulation. The

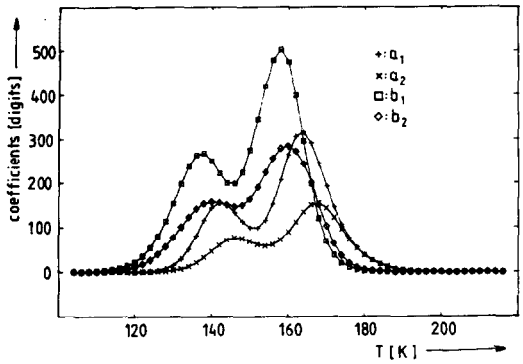

Fig. 7. Calculated Fourier temperature scan at overlap of transients of two trap levels; $N = 256$, $\Delta t = 1$ ms.

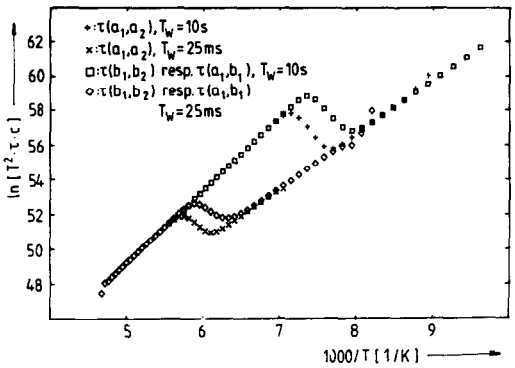

Fig. 9. Arrhenius plot for two different period widths.

curves of each coefficient show two relative maxima. The Arrhenius plot (Fig. 8) exhibits a transition between two straight lines. Due to the overlapping of two transients the evaluation is limited to a smaller temperature range. Several methods can be used to overcome this reduction.

First, the existence of two exponential functions means that the equation for the transient contains four unknown quantities, 2 amplitudes and 2 emission time constants. With 4 coefficients a non-linear equation system can be solved. A second possibility of correction utilizes the fact that the maxima of the different coefficients in Fig. 7 are displaced in relation to each other. Thus, to evaluate one level one uses coefficients which are less affected by the other one. As the maxima of the cosine coefficients a_n occur at higher temperatures one chooses a_1 and a_2 for the evaluation of the shallower trap level (faster transient) in the transit region, i.e. $\tau(a_1, a_2)$. For the transient with the larger emission time constant one uses $\tau(b_1, b_2)$. The resulting activation energies are 0.269 and 0.361 eV, the capture cross sections 1.8×10^{-14} and $5.3 \times 10^{-13}\,\mathrm{cm}^2$.

There is a third way for correction. As a change of period width shifts all maxima on the temperature axis, it is of advantage to carry out 2 transformations for different period widths. Within the transit region

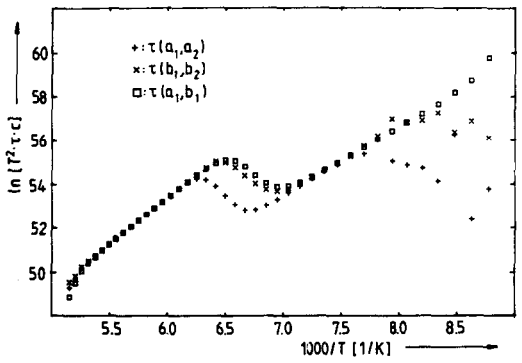

Fig. 8. Arrhenius plot for Fig. 7.

coefficients of large period width are chosen for the slow transient, while for the fast signal the coefficients of short period width are used. If the appropriate τ-ranges are combined the range to be evaluated can be extended remarkably (Fig. 9). Even better results are achieved when t_0 and T_W—in accordance with the changes of the two transients—are varied during measurement. If one chooses for measuring transient 2 (larger emission time constant) $t_{02} \approx t_{01} + T_{W1}$, and a period width where b_1 and b_2 are maximal for transient 2, then the effect of transient 1 (smaller emision time constant) on $\tau(b_1, b_2)$ is negligible. Even if the parameter choice is not optimal, it is still guaranteed that the interference will be small because a fast signal affects mostly the cosine coefficients. For measuring transient 1, a period width is chosen that a_1 and a_2 yield maximal values. If the 2nd signal is substantially slower than the 1st then the cosine coefficients of transient 2 are nearly zero at the period width T_{W1}. $\tau(a_1, a_2)$ will then produce the undisturbed emission time constant of the first transient. If the two emission time constants differ only slightly an effect by the 2nd exponential function cannot be excluded even at this short observation time. Even then the calculation of the larger emission time constant is nearly exact and can be used to correct the smaller emission time constant:

$$a'_{n1} = a_{n1} - b_{12}\frac{T_{W2}}{T_{W1}}\exp\left(\frac{t_{02} - t_{01}}{\tau_2}\right) \times \frac{[1 - \exp(-T_{W1}/\tau_2)]}{[1 - \exp(-T_{W2}/\tau_2)]} \times \frac{1/\tau_2^2 + \omega_2^2}{1/\tau_2^2 + n^2\omega_1^2}\frac{1}{\tau_2\omega_2}, \tag{15}$$

with a_{n1} = cosine coefficients of measurement 1; b_{12} = 1st sine coefficient of the 2nd measurement; a'_{n1} = corrected cosine coefficients for measurement.

The a'_{n1} coefficients should contain only parts of the 1st transient. From these coefficients $\tau(a_1, a_2)$ can now be calculated. Figure 10 shows a simulation carried out in this way. For a large temperature range both emission time constants can be evaluated ex-

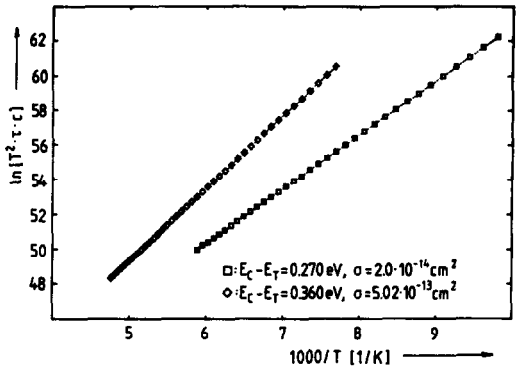

Fig. 10. Arrhenius plot of two levels at variable period width.

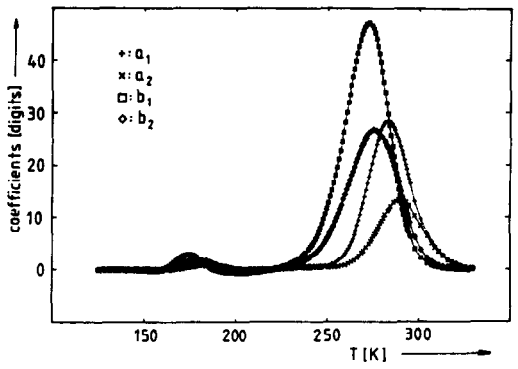

Fig. 12. Fourier temperature scan of a Si-*pn*-diode for $N = 256$ and $\Delta t = 0.1$ ms.

actly. This method allows to separate two time constants which differ by a factor of two, if equal amplitudes can be assumed.

5. MEASUREMENTS

5.1. Si-pn-diode

The block-diagram of the DLTFS system is shown in Fig. 11. To compare the DLTFS method with the conventional technique, measurements for known samples have been performed.

Figure 12 shows the measured DLTFS-temperature curves of a gold doped p^+-n-Si-diode. The shallow donor concentration was $2 \times 10^{14}\,cm^{-3}$. Even at small values the curves satisfy the assumption of optimal noise suppression. To extend the temperature range which can be used for the determination of the activation energy as large as possible, a measurement with variable parameters was carried out. The direct calculation of the emission time constant as well as its verification allows the calculation of the activation energy already during measurement. The t_s/T_W-setting uses the preliminary result to pre-calculate the emission time constant for the next measuring point. However, the exact value of T_W is not critical as not only one value but a relatively wide range is possible for this. Evaluation of the measuring result also fixes the temperature at which the following measurement should take place.

Controlled by a heating program, the temperature is increased slowly in the range with measurable transients. Otherwise the temperature is quickly increased. One advantage of this is that measuring time is saved, the other is that a large number of τ-calculations can be done in the temperature range of interest. Because each of these measurements also contributes a point to the Arrhenius plot, the exactness of the evaluation can be increased. For the DLTS method, however, the maximum number of points for the Arrhenius plot is limited by the number of rate windows.

In Fig. 13 the squares represent the b_1-coefficient with $N = 1024$ and $\Delta t = 0.1$ ms, obtained from the numerical transformation. For measurements with a smaller period width, the resulting values for A and τ were used to calculate b_1 of the above period, according to eqn (11). These theoretical values are marked by triangles in Fig. 13. With the data obtained via the Arrhenius plot the development of the coefficients for the acceptor level were theoretically re-calculated (straight line). The good agreement of all three curves—except for the peripheral points—argues well for the accuracy of the results.

Figure 14 shows the Arrhenius plot for this measurement. The various τ-calculations lead to nearly identical results: the activation energy is 0.564 eV, the capture cross section $3.1 \times 10^{-14}\,cm^2$, and the trap concentration $9 \times 10^{12}\,cm^{-3}$.

For comparison the *pn*-diode has been measured

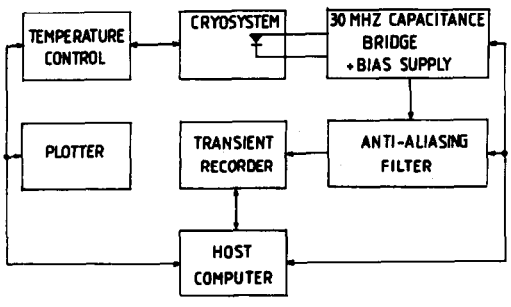

Fig. 11. Block-diagram for the DLTFS system.

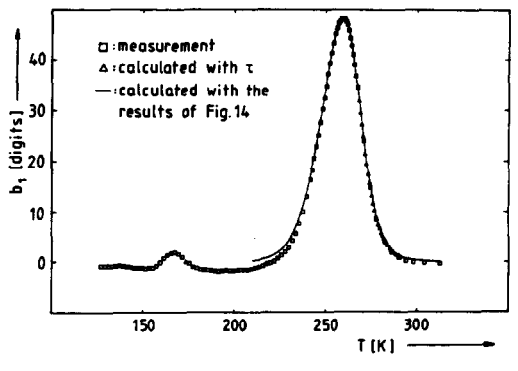

Fig. 13. b_1-temperature scan of Si-*pn*-diode for $N = 1024$ and $\Delta t = 0.1$ ms.

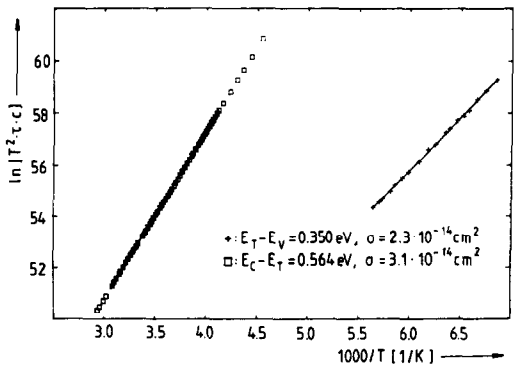

Fig. 14. Arrhenius plot of the gold acceptor and the gold donor level in Si for the DLTFS-measurement.

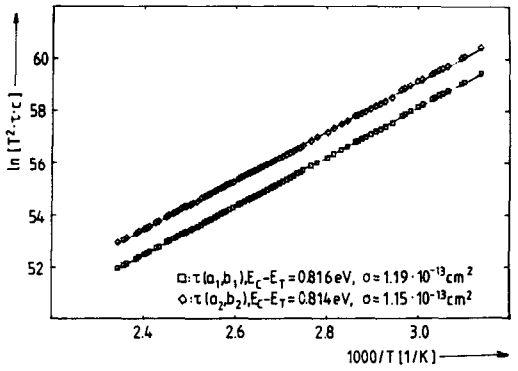

Fig. 16. Arrhenius plot for n-GaAs; the values of $\tau(a_2, b_2)$ are displaced parallel by 1 unit of the ordinate axis.

also using conventional techniques. The noise suppression was considerably worse. With the obtained values of 0.602 eV for the energy and 1.07×10^{-13} cm^2 for the capture cross section (Fig. 15) the measured temperature scans could not be fitted. The explanation for this fact is that the amplitude of the transients during this charging of the deep level increases with the temperature and the negative values are obtained for the coefficients in the temperature scan.

Although the signal/noise ratio is often 1, the transients of the donor level could still be evaluated with the DLTFS method. Figure 14 was used to obtain a value of 0.350 eV for the energetic position, and 2.3×10^{-14} cm^2 for the capture cross section.

5.2. n-GaAs-Schottky-contact

Figure 16 shows the Arrhenius plot of a CC (Constant-Capacity)-DLTFS measurement of a n-GaAs-Schottky-diode in the temperature range from 300 to 430 K. For $\tau(a_2, b_2)$ the curve is shifted upward by 1 unit to achieve greater clarity. Despite the straight lines being hardly distinguishable, the evaluation resulted in some differences. Thus for the activation energy values of 0.816 respectively 0.814 eV, and 1.19×10^{-13} respectively 1.15×10^{-13} cm^2 for the capture cross section were determined.

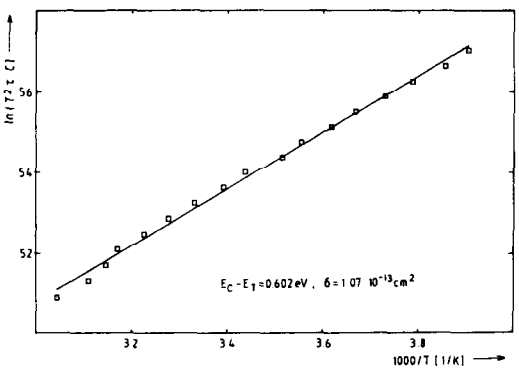

Fig. 15. Arrhenius plot of the gold acceptor level for the DLTS-measurement.

An explanation for this behaviour is found by a direct comparison of the emission time constants for the various calculation methods. For these, systematic differences can be found depending on the position of the transient with respect to the period width. This means that the signal was not a real exponential. Measurements at constant voltage showed the effect more clearly than CC-DLTFS-measurements. The reason for this effect is most likely to be found in the fact that $N_T/N_S \ll 1$ does not hold[8]. The influence of the large trap concentration can be reduced by optimal setting of period width, and appropriate choice of τ-calculation for a CC-DLTFS-measurement.

The measurements for GaAs-Schottky-diodes are clearly proving the sensitivity of the DLTFS method. Although no anomalies can be found by optical inspection of the temperature scan, Arrhenius plot, and transients, systematic effects occurred in the τ-calculation resulting from not purely exponential transients.

6. DISCUSSION

In the following the conventional DLTS method, as described in the Introduction, will be compared with the DLTFS method.

(a) In the DLTFS method the experimental set-up is more complex than in the DLTS system, because a transient recorder as well as a fast computer are necessary. The software is much more complex, too. The advantage of this expense is of course, that the whole transient is measured and that a completely computer controlled digital system is available for the measurement itself as well as for its evaluation.

(b) If the time constant in the DLTFS method is determined from the maxima of the Fourier temperature curves in analogous to the DLTS method, both methods yield the same energy resolution for the separation of two adjacent levels. However, if the time constant is evaluated directly from the Fourier

coefficients, as described in this paper, the energy separation of neighbouring levels is worse than in the DLTS method. It is possible that the amplitude of the Fourier coefficients or their ratio is largely affected from an adjacent level, but the position of the maxima of the coefficients remains mainly constant. However, if a correction is possible, as described in Section 4.2, the DLTFS method results in a higher energy resolution.

(c) The DLTFS method has a better noise suppression in practice. With only the Fourier coefficients of the first order being evaluated, the conventional DLTS and the DLTFS method (at identical measuring times $t_2 = T_W$) possess—in theory—the same "band width" $1/t_2 = 1/T_W$ (analog/digital filtering). To meet the requirements of the sampling theorem an analog filter has to cut-off the frequencies above $1/t_2$ and $1/(2\Delta t)$, respectively. Here the DLTS method places a much higher demand on the analog filter than the DLTFS method with regard to frequency response, phase response and response time. For instance, the response time (reversely proportional to the filter frequency) does not allow adjustment of the best filter frequency, as given from the sampling theorem, if the conventional method is used. The DLTFS method, however, obtains this frequency by the Discrete Fourier Transformation. The response time of a digital filter is of no importance because the transient is not reconstructed.

Furthermore, by varying the number of measuring values during the evaluation, several first order coefficients of various basic frequencies can be calculated from a single transient, and each will possess the optimal signal-noise ratio (SNR). This contrasts the DLTS method where the analog filter for a transient can be adjusted optimally for one rate window only, because this filter cannot be adjusted during measurement of the whole transient.

With the DLTFS method the determination of the time constant is necessary at only one period width, i.e. at only one "rate window", and this is adjusted to the decay length of the transient. Thus, each temperature measuring point has an optimal SNR, and the shortest measurement time possible according to the measuring conditions. The time saved can be used for repeated averaging, and, therefore, for a better noise suppression.

(d) Using the so-called conventional evaluation it is assumed in eqn (1), that only the emission time constant in the $C(t)$-transient depends on temperature. However, this is only valid if the amplitude of the exponential function remains constant throughout the entire measurement. With the DLTFS method, on the other hand, the calculations of time constant and amplitude are independent of each other. Therefore, a temperature dependence of the amplitude does not present a source of error for the evaluation. This advantage is especially important with current DLTS measurements.

(e) The characteristic quantities of the trap level are obtained via an Arrhenius plot. However, the linearity of the Arrhenius plot is a relatively insensitive proof for the validity of the evaluation; especially, as the linearity is not an unequivocal confirmation of an exponential transient as was postulated for eqn (1). Hence, with a conventional evaluation, the results obtained must be used to recalculate the temperature curves, and these, in turn, must be compared with the curves obtained experimentally. The DLTFS method, however, checks the postulated law of time right at the evaluation of the time constant. Thus, a recalculation of the temperature curves is unnecessary.

(f) The DLTFS method does not evaluate the time constant via the maxima of the temperature curves but derives time constant and amplitude for each measuring point in a different manner allowing control of the results. This simplifies evaluation and facilitates automation. It also allows an evaluation during measurement and therefore a complete control of parameters. The temperature of the next measurement can be set according to the results obtained, thus resulting in a speeding-up of the entire measuring process. Generally, the period width and consequently the measurement time at each temperature point is chosen according to the decay behaviour of the transient by the measuring program. It is possible to obtain an "extrapolation" of the characteristic quantities of the deep level during the measurement.

(g) While the conventional evaluation of the complete temperature scan of a single rate window yields just one point of the Arrhenius plot, with the DLTFS method each temperature point with an evaluable transient contributes to the Arrhenius plot.

7. CONCLUSIONS

In this paper we have presented the main characteristics and advantages of the DLTFS technique for measurements on discrete levels. A further publication will show how interface state characteristics of MIS-capacitors as well as generation of minority carriers can be investigated with this technique. Especially an identification of inversion build-up is possible. Furthermore, the advantages of the DLTFS method for calculation of depth profiles will be described. Field dependences of the time constant can be recognized very easily, and their influences can be kept low in most cases. Additionally, a new type of capture measurement will be presented.

REFERENCES

1. W. Shockley and W. T. Read, *Phys. Rev.* **87**, 835 (1952).
2. D. V. Lang, *J. appl. Phys.* **45**, 3014, 3023 (1974).
3. D. V. Lang, *Space-Charge Spectroscopy in Semiconductors* (Edited by P. Bräunlich). Springer, Berlin (1979).

4. R. Kassing, L. Cohausz, P. van Staa, W. Mackert and H. J. Hoffmann, *Appl. Phys.* **34,** 41 (1984).
5. K. Ikeda and H. Takaoka, *Jap. J. appl. Phys.* **21,** 462 (1982).
6. P. D. Kirchner, W. J. Schaff, G. N. Maracas and L. F. Eastman, *J. appl. Phys.* **53,** 6462 (1981).
7. M. Okuyama, H. Takakura and Y. Hamakawa, *Solid-St. Electron.* **26,** 689 (1983).
8. M. Bleicher and E. Lange, *Solid-St. Electron.* **16,** 375 (1973).